Optics Communications 516 (2022) 128266

Contents lists available at ScienceDirect

Optics Communications

journal homepage: www.elsevier.com/locate/optcom

Demonstration of all-digital burst clock and data recovery for symmetrical 50 Gb/s/λ PON based on low-bandwidth optics

Jiao Zhang [a,b], Qingyi Zhou [a], Min Zhu [a,b,*], Bingchang Hua [b], Mingzheng Lei [b], Yuancheng Cai [a,b], Liang Tian [b], Yucong Zou [b]

[a] National Mobile Communications Research Laboratory, Southeast University, Nanjing 210096, China
[b] Purple Mountain Laboratories, Nanjing 211111, China

ARTICLE INFO

Keywords:
Passive optical networks (PONs)
Pulse amplitude modulation (PAM)
Burst clock and data recovery (BCDR)
Uplink burst-mode transmission

ABSTRACT

We experimentally demonstrated all-digital burst clock and data recovery (BCDR) for symmetrical single-wavelength 50 Gb/s four-level amplitude modulation (PAM-4) passive optical network (PON) over the same fiber link at O-band, with the using of 10G-class optics and simple digital signal processing (DSP). The uplink burst frame and BCDR algorithm is used for accurately evaluating PON uplink transmission performance. The results show that over 26 dB link loss budget for continuous-mode uplink transmission and over 25 dB for burst-mode uplink transmission at a bit error rate of 3.8×10^{-3} can be achieved, respectively. For symmetrical 50 Gb/s/λ PON uplink burst-mode, there are 1 dB power budget loss less than uplink continuous-mode.

1. Introduction

Driven by the rapid development of cloud services, business services, and 5G wireless backhaul, the ever increasing capacity demands of access network grows pretty fast. Passive optical networks (PONs) are deployed worldwide as a cost-effective technology for access networks [1]. The IEEE 802.3ca Task Force has released 25 Gb/s and 50 Gb/s Ethernet PON (EPON) standards by bonding two wavelength channels to reach its 50 Gb/s target [2], and the ITU-T single wavelength 50 Gb/s PON in project G. hsp took a big step towards becoming a reality as consent during the ITU-T SG15 plenary meeting on April 23, 2021 [3]. Four-level amplitude modulation (PAM-4) is the most potential modulation format for high-capacity PON systems due to its simpler digital signal processing (DSP) architecture and lower energy consumption [4]. There have been several works on demonstration of 50G PON by using the PAM-4 as the modulation formats for the next generation PON [5–8]. In [6,8], the downlink and uplink for a symmetrical PON are separately studied with different fiber links. The transmission between the two links is independent. Besides, in these works, the uplink transmission is studied in continuous-mode, without considering data burst-mode. The transceivers in optical links require a high speed clock and data recovery algorithm to extract a synchronous clock and recover the received data. While for the upstream in PONs with the symbol rate of 25 GBaud, the fast synchronization remains a significant technical challenge due to the burst-mode nature of the traffic. A sufficiently short settling time is required to ensure the data is correctly recovered. Burst clock and data recovery (BCDR) has not yet been reported on symmetrical single-wavelength 50 Gb/s PAM-4 PON over the same fiber link based on bandwidth limited optics.

Various BCDR techniques have been proposed for Non-Return-to-Zero (NRZ)signals, such as phase locked loops (PLL), gated-voltage controlled oscillators (G-VCO) and over-sampling [1,9]. Several research works have been reported for BCDR in PON upstream link. In [10], 10.3 Gb/s burst-mode 3R receiver incorporating a full automatic gain control optical receiver and 82.5-GS/s over-sampling clock and data recovery (CDR) for 10G-EPON was developed, and the receiver sensitivity of −30.1 dBm at the BER of 10^{-3} and the upstream power budget of 37.6 dB are successfully achieved. In [11], a hybrid burst-mode CDR employing high-speed samplers and a G-VCO was presented for 10Gbps PON and a large tolerance to the pulse distortion over 0.64 unit interval (UI) was successfully shown with the G-VCO supported half-rate sampling technique. However, the G-VCO CDR has the disadvantages of no jitter rejection and reduced pulse-width distortion (PWD) tolerance [12]. The over-sampling CDR suffers from high power consumption and large integrated circuit (IC) chip area [13,14]. The PLL implementations rely on analog building blocks and require too many transitions to lock [15,16]. For PAM-4 signals, traditional methods are more challenging, since there are more transition types for PAM-4 signal than for NRZ signal. Instead, an all-digital phase detection and interpolation-based CDR can avoid such a complicated setup, allowing a free-running analog-to-digital converter (ADC) and ensuring a fast CDR for base-band signals [17,18]. Among many all-digital re-timing algorithms, the squaring timing recovery as

* Corresponding author at: National Mobile Communications Research Laboratory, Southeast University, Nanjing 210096, China.
E-mail address: minzhu@seu.edu.cn (M. Zhu).

https://doi.org/10.1016/j.optcom.2022.128266
Received 24 October 2021; Received in revised form 24 February 2022; Accepted 30 March 2022
Available online 4 April 2022

a feed-forward, non-data-aided method, can be implemented efficiently for clock phase estimation due to the high loop bandwidth [17,19]. Input signal is sampled at a fixed rate by a free running oscillator and absolute timing offset is determined from the given samples of the signal by BCDR for symbol detection to recover the burst clock and data [17].

In this paper, all-digital BCDR for symmetric single-wavelength 50Gb/s PAM-4 PON uplink burst transmission based on bandwidth limited optics has been experimentally demonstrated. Instead of traditional continuous-mode uplink, burst-mode upstream link is utilized in PON transmission for more accurate evaluation. This is the first BCDR demonstration for symmetric 50 Gb/s/λ PAM-4 PON downstream and upstream over the same fiber link at O-band. First, we elaborate on the principle of BCDR based on squaring timing recovery algorithm. Subsequently, the setup of a symmetric 50G PON uplink burst transmission system based on bandwidth limited devices is presented. Then, the uplink burst frame is designed based on the system. Finally, the performance of downlink continuous-mode and uplink burst-mode transmission are discussed, respectively. The results show that the evaluation of symmetrical 50 Gb/s/λ PON performance by uplink burst-mode has 1 dB power budget loss less than uplink continuous-mode.

2. Principle of BCDR based on squaring timing recovery algorithm

In current high-speed optical fiber transmission system, the optical signal is converted into an electrical signal by photoelectric detection, and then digitized by an ADC. However, the sampling clock of the receiver is unsynchronized to that of the transmitter, so the non-optimal sampling point of ADC will lead to sampling clock error. BCDR is used to eliminate the influence of sampling clock error in the experimental system. BCDR for optical fiber transmission mainly includes Gardner and squaring timing recovery algorithm. There is time delay in the feedback structure used by Gardner timing recovery. However, as a feedforward, non-data-aided method, the squaring timing recovery is efficient for high-speed burst signals due to faster timing synchronization speed. Hence, we adopted the BCDR algorithm based on squaring timing for burst mode upstream link in symmetric 50 Gb/s/λ PON transmission.

Here we assume that the timing recovery for digital data transmission is linear modulation scheme, and the received PAM signal can be expressed as [17]

$$r(t) = \sum_{n=-\infty}^{\infty} a_n g_T(t - nT - \varepsilon(t)T) + n(t), \tag{1}$$

where a_n is the value of transmitted PAM symbols, $g_T(t)$ is the transmission signal pulse, T is the symbol duration, $n(t)$ is the White Gaussian noise, and $\varepsilon(t)$ is an unknown and slowly varying time delay.

In digital realization, the received PAM signal can be processed step by step because of the slow variation of $\varepsilon(t)$. For each section, we can assume ε to be constant. After a receiving filter with an impulse response of $g_R(t)$, the received signal can be written as

$$\bar{r} = r(t) * g_R(t), \tag{2}$$

where "$*$" is the convolution symbol. The filtered signal is sampled at rate N/T. We thus have samples as follow

$$r_k = r\left(\frac{kT}{N}\right) = \sum_{-\infty}^{\infty} a_n g\left(\frac{kT}{N} - nT - \varepsilon T\right) + n\left(\frac{kT}{N}\right), \tag{3}$$

here $g(t) = g_T(t) * g_R(t)$ is the total response of transmission signal and filter. Then the sampled signal is modulo squared, which can be expressed as

$$x_k = |r_k|^2, \tag{4}$$

the sampled sequence contains a spectral component at $1/T$. The spectral component is determined for every section of length LT by calculating the complex Fourier coefficient at the symbol rate

$$X_m = \sum_{k=mLN}^{(m+1)LN-1} x_k e^{-j2\pi k/N}, \tag{5}$$

the normalized phase of this coefficient is an unbiased estimate for $\hat{\varepsilon}_m$ as follow

$$\hat{\varepsilon}_m = -\frac{1}{2\pi} \arg\left(X_m\right). \tag{6}$$

In addition, the sampling rate of the receiver needs to meet the requirement of $N/T > 2/T$ in order to ensure that the spectral component at $1/T$ can be extracted correctly. In the case of bandwidth efficient modulation, the single-sided bandwidth of transmission signal is less than $1/T$ and the single-sided bandwidth of $g_R(t)$ before receiver is also less than the symbol rate. Then the squared signal should have a single-sided bandwidth of less than $2/T$. Therefore, with $N = 4$, the sequence $x_k(t)$ completely describes the continuous time signal $x(t)$.

3. Experimental setup

Fig. 1 shows the experimental setup for symmetrical 50 Gb/s/λ PAM-4 PON transmission based on bandwidth limited optics in the O-band, with the use of simple DSP and semiconductor optical amplifiers (SOAs). The downlink and uplink signals are separated by optical couplers (OC-1 and OC-2) and transmitted in the same optical fiber link. For both downlink and uplink, the 25 GBaud PAM-4 signal is generated and performed offline by MATLAB and uploaded into a 64GSa/s arbitrary waveform generator (AWG) used as a digital-to-analog converter (DAC), and then amplified by a 25 GHz linear electrical amplifier (EA) before signal modulation. For the downlink, a commercial O-Band directly modulated laser (DML-1) is used with center wavelength of 1314.944 nm, and output power of 9.62 dBm. Then, the modulated optical signal is transmitted over 20 km standard single-mode fiber (SSMF) with an average loss of 0.33 dB/km at 1310 nm. A variable optical attenuator (VOA-1) is placed after SSMF to simulate the splitter loss. To support a larger link loss budget, a semiconductor optical amplifier (SOA-1) at the ONU is used as a pre-amplifier before direct detection. An isolator (ISO-1) is placed between VOA-1 and SOA-1 to avoid light reflection. VOA-2 is deployed to adjust the received optical power (ROP) for sensitivity measurement. Integrated PIN and TIA is used for signal detection after pre-amplification. After signal detection, the signal is captured by a 100GSa/s digital storage oscilloscope (DSO) with 33 GHz bandwidth for further offline DSP. For the uplink, the baseband PAM-4 signal is directly modulated by another commercial DML-2 at the center wavelength of 1299.518 nm. The output power of the DML-2 is 9.3 dBm. In addition, the performance parameters of the devices, such as VOA-3, ISO-2, SOA-2 and VOA-4, used in the uplink are the same as the downlink. All commercially available SOAs (Thorlabs, BOA1132LR) have the same device characteristics with a small-signal gain of 30 dB, a noise figure of 7 dB and a saturation output power of 17 dBm. The polarization dependent gain of both SOAs is less than 1 dB.

For both downstream and upstream links, 10 Gb/s commercial DML is used at transmitter side, and integrated PIN-TIA is used at receiver side with 15 GHz optical bandwidth and 11 GHz electrical bandwidth. The frequency response of the transceivers is shown in Fig. 2(a) and (b). It can be seen that the bandwidth of the system increases with the increase of the driving current. At high driving current, DML can suppress the transient chirp and improve the dispersion tolerance to support longer fiber transmission, but the high extinction ratio (ER) cannot be achieved, thus limiting the receiver sensitivity of the signal. After comprehensive consideration, 65 mA current was chosen to drive DML for the experiment. According to the measured results, the 3 dB and 10 dB bandwidth of the downstream transceivers are 17.4 and 23 GHz, respectively. As shown in Fig. 2(b), the 3 and 10 dB bandwidth

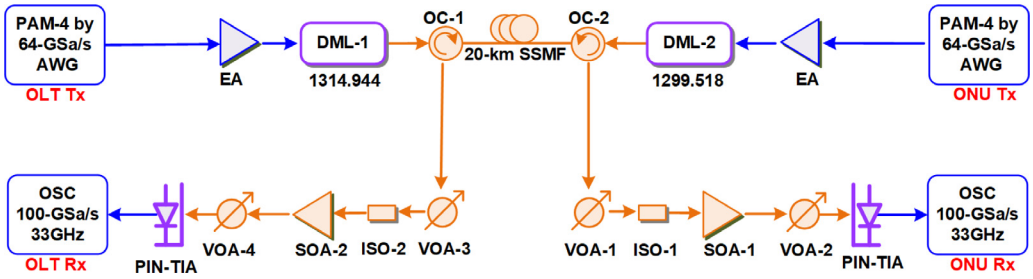

Fig. 1. Experimental setup of symmetrical 50 Gb/s/λ PON based on low-bandwidth optics over the same fiber link at O-band.

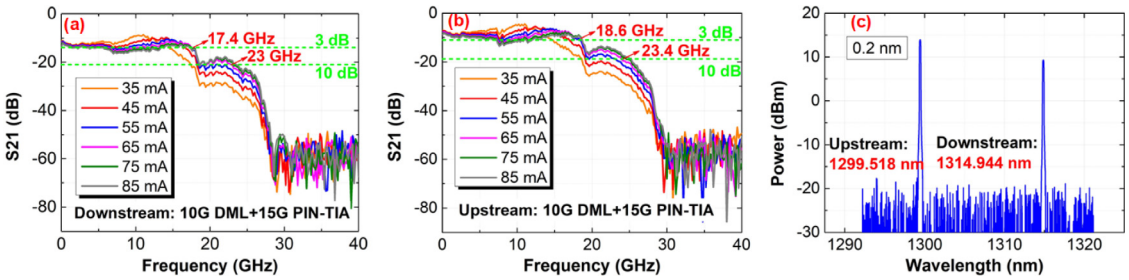

Fig. 2. The frequency response of the transceivers of 10G DML and 15G PIN-TIA for (a) downlink and (b) uplink. (c) Optical spectra of downlink and uplink.

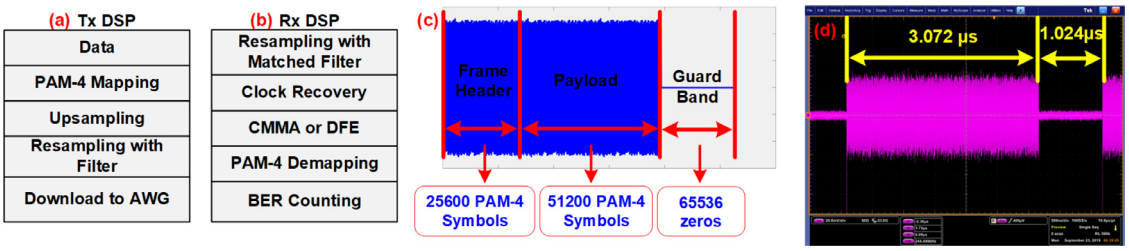

Fig. 3. (a) and (b) are the offline DSPs for PAM-4 signal generation and recovery, respectively. (c) The structure of uplink burst frame. (d) The duration of uplink burst frame captured by oscilloscope.

of the upstream transceivers are 18.6 and 23.4 GHz, respectively. The optical spectra of downlink and uplink are also given in Fig. 2(c). The central wavelength of downlink is 1314.944 nm, and that of uplink is 1299.518 nm.

Fig. 3(a) and (b) show the offline DSPs for PAM-4 signal generation and recovery, respectively. For continuous mode downstream link, the detailed transmitter offline DSP includes pseudo-random bit sequence (PRBS), PAM-4 mapping, up-sampling, shaping filtering, resampling and normalization. The corresponding PRBS length of Gray-mapped PAM-4 symbols is 2^{15}. At the Rx DSP, the captured offline data is firstly resampled to 2 samples per symbol and then processed by a matched filter to reduce out-of-band noise [8]. After that, a squaring time recovery is performed to remove timing offset and jitter from the data. Linear equalization based on cascaded multi-modulus algorithm (CMMA) or decision feedback equalizer (DFE) is used before bit error ratio (BER) calculation. As a blind equalization algorithm, CMMA equalizer can obtain channel characteristics by sending statistical channel information without additional training sequence, and calculate the output error by using multiple cascaded constant modes. The tap weights of DFE are adaptively updated by decision-directed least mean square (DD-LMS) algorithm.

For burst mode upstream link, the structure of burst frame is shown in Fig. 3(c), which consists of three parts: frame header, payload and guard band. Here in our demonstration, the frame header is designed with 25600 PAM-4 symbols for clock synchronization and data recovery. 51200 PAM-4 symbols are used as payload, and 65536 zeros are used as guard band between frames. The generation of PAM-4 signal in uplink burst mode is consistent with that in downlink continuous mode. Fig. 3(d) shows the uplink burst frame captured by oscilloscope. The duration of data is 3.072 μs, and the guard band is 1.024 μs. BCDR based on squaring timing recovery algorithm is used to recover the uplink burst data clock at receiver side. In addition, there are no pre-distortion methods such as digital pre-equalization and lookup table (LUT) pre-distortion methods at the transmitter side, and neither nonlinear equalization such as volterra nonlinear equalization (VNE) at receiver side to simplify the DSP process and reduce the complexity [20].

4. Results and discussions

4.1. Downlink continuous-mode transmission

The system optimization is first performed in order to find the suitable equalization algorithm and taps number. The BER performance versus different taps number at different received optical power (ROP) with CMMA or DFE equalization are presented in Fig. 4. We find that increasing the taps number of equalization algorithm is an effective way to further improve BER performance. The improvement effect is more obvious at high ROP. The performance improvement of the two equalization algorithms is similar, and both are stable when the number of equalization exceeds 50 taps. In order to further verify the system performance, 99-tap CMMA are chosen for the downlink continuous-mode transmission.

Based on the system device and DSP parameters discussed above, the BER performance of 50 Gb/s PAM-4 PON versus ROP for downlink

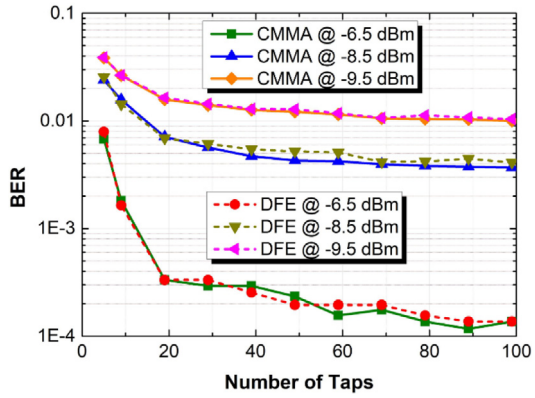

Fig. 4. The BER performance versus the taps number of CMMA and DFE at different ROP.

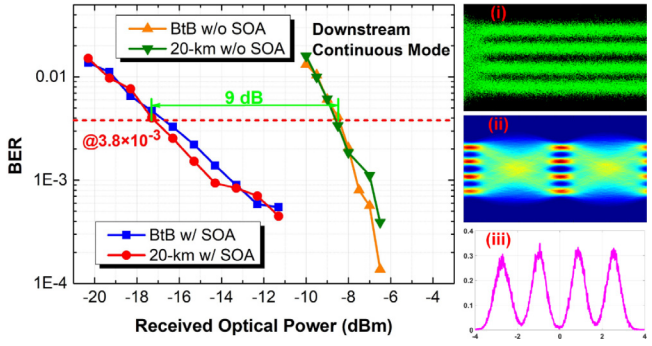

Fig. 5. The BER performance versus ROP for downlink continuous-mode. Insets (i)-(iii) are recovered symbols, eye diagram and histogram under the BER threshold at 3.8×10^{-3}.

continuous-mode without and with 20 km fiber transmission are shown in Fig. 5. VOA-2 is deployed to adjust the received optical power ROP for sensitivity measurement. The bias current optimized by SOA is set at 200 mA and the power into PIN-TIA is fixed at about 3 dBm. It should be noted that the BCDR algorithm must be used for clock recovery in the downlink transmission, otherwise the signal cannot be recovered stably. As shown in Fig. 5, the receiver power after 20 km fiber transmission without SOA at HD-FEC (3.8×10^{-3}) and SD-FEC (1×10^{-2}) threshold are −8.3 dBm and −9.5 dBm, respectively. In this case, the power budget is not enough to meet the requirements of PON system. The receiver sensitivity is −17.3 dBm and −19.3 dBm at the HD-FEC threshold and SD-FEC threshold with SOA, resulting in 26.92 dB and 28.92 dB power budget with 9.62 dBm DML output power. Around 9 dB and 8.8 dB power budget improvement can be achieved by using SOA at HD-FEC and SD-FEC threshold. There is no obvious dispersion penalty after 20 km transmission due to near zero-dispersion wavelength of DML. Insets (i)-(iii) are recovered symbols, eye diagram and histogram at −17.3 dBm ROP, respectively. It can be observed that the signal was clearly recovered after CMMA from the eye diagram. According to the histogram, we can see the standard distribution of the four amplitude levels of PAM-4, and each level shows a distribution like Gaussian.

4.2. Uplink burst-mode transmission

We initially investigated the BER performance versus the clock recovery symbols of CMMA and DFE with BCDR before uplink burst-mode transmission experiment, as shown in Fig. 6. The taps number of 99 is used for CMMA and DFE. We find that increasing the PAM-4 symbols for clock recovery is an effective way to further improve

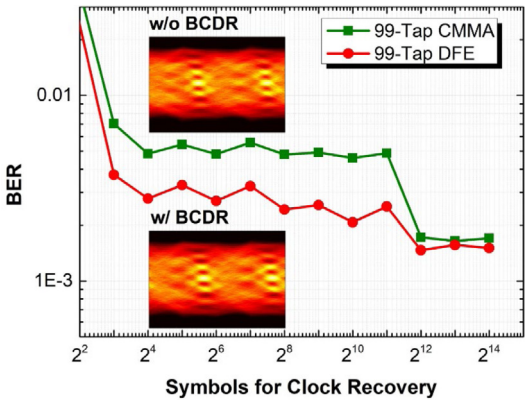

Fig. 6. The BER performance versus the clock recovery symbols of CMMA and DFE with BCDR..

BER performance of 50 Gb/s PON. The symbol length of 2^{12} is enough to stabilize the system performance because the clock of the signal is estimated sufficiently. In addition, the performance of DFE outperforms CMMA after using BCDR when the number of clock recovery symbols is small. The performance of both is similar when the number of clock recovery is up to 2^{12} symbols, with DFE slightly superior to CMMA. Here in our design, 25600 PAM-4 symbols are used as frame header, sufficient for burst clock and data recovery. Therefore, in the experiment of uplink burst-mode transmission of symmetrical 50G PAM-4 PON based on bandwidth-limited optics, 99-tap DFE is used for digital signal equalization. The illustrations in Fig. 6 show the PAM-4 eye diagrams of PAM-4 without and with BCDR, respectively. It can be seen that the eye diagrams of the signal are skew due to the frequency chirp, and it becomes clear with the use of BCDR.

We also test the BER performance of uplink burst-mode versus ROP, as shown in Fig. 7. Based on the burst frame designed above, the receiver power of −7.3 dBm and −9 dBm are obtained after 20 km fiber transmission without SOA at HD-FEC and SD-FEC threshold, respectively. The achieved receiver sensitivity for the HD-FEC threshold and SD-FEC threshold are −16.3 dBm and −19 dBm by using SOA, resulting in 25.62 dB and 28.32 dB power budget. Therefore, by using SOA, 9-−10 dB optical gain can be obtained. Most studies on uplink transmission have only been reported for continuous mode. In order to compare performance in uplink burst mode and uplink continuous mode, uplink continuous-mode for 20 km fiber transmission is tested in Fig. 7. As we can observe, the performances of uplink burst-mode have around 1 dB loss compared to continuous-mode case. Insets (i) shows that the PAM-4 signal frame cannot be recovered without the use of BCDR in uplink burst-mode transmission. Insets (ii) is captured uplink burst frame with BCDR, and it can be observed that stable clock recovery is achieved by using the squaring timing recovery algorithm. Inset (iii) is clear eye diagram of the recovered 25 Gbaud PAM-4 signal.

5. Conclusions

In this paper, all-digital BCDR for symmetrical single-wavelength 50-Gb/s PAM-4 PON over the same fiber link at O-band, with the using of 10G DML and 15G PIN-TIA and simple DSP is experimentally demonstrated for the first time. The performances of uplink burst-mode compared with uplink continuous-mode are also evaluated. Instead of continuous-mode uplink, burst-mode upstream link is more accurate evaluation in practical PON transmission. Over 26 dB power budget for continuous-mode downlink transmission at HD-FEC threshold and over 25 dB link loss budget for burst-mode uplink transmission can be achieved at HD-FEC threshold. The performance of uplink burst-mode is around 1 dB less than uplink continuous-mode.

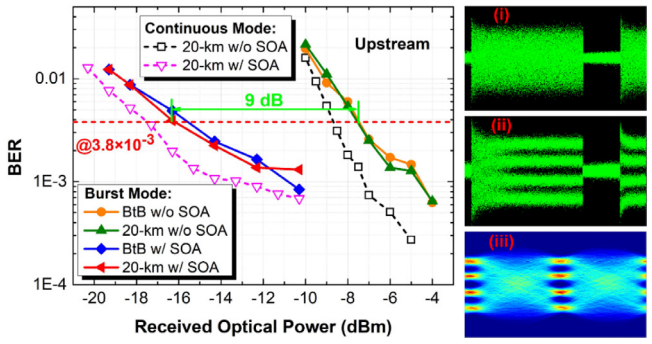

Fig. 7. The BER performance versus ROP for uplink burst-mode. Insets (i)-(ii) are recovered symbols without and with BCDR. Inset (iii) is eye diagram of recovered signal.

Declaration of competing interest

The authors declare that they have no known competing financial interests or personal relationships that could have appeared to influence the work reported in this paper.

Acknowledgment

This work was partially supported by National Natural Science Foundation of China (62101121, 62101126), China Postdoctoral Science Foundation (2021M702501), Transformation Program of Scientific and Technological Achievements of Jiangsu Province, China (BA2019026), and Key Research and Development Program of Jiangsu Province, China (BE2020012).

References

[1] X. Qiu, X. Yin, J. Verbrugghe, B. Moeneclaey, A. Vyncke, C. Van Praet, et al., Fast synchronization 3R burst-mode receivers for passive optical networks, J. Lightw. Technol. 32 (2014) 644–659.
[2] IEEE 802.3ca task force, 2021, [Online]. Available: http://www.ieee802.org/3/ca/index.shtml. (Accessed 25 January 2021).
[3] https://www.itu.int/ITU-T/workprog/wp_item.aspx?isn=14550.
[4] N. Kikuchi, R. Hirai, Intensity-modulated/ direct-detection (IM/DD) nyquist pulse-amplitude modulation (PAM) signaling for 100-Gbit/s/λ optical short-reach transmission, in: Proc. ECOC, 2014, pp. 1–3.
[5] X. Miao, M. Bi, J. Yu, L. Li, W. Hu, SVM-modified-FFE enabled chirp management for 10G DML-based 50gb/s/λ PAM4 IM-DD PON, in: Proc. Optical Fiber Communication Conference, 2019, M2B.5.
[6] K. Zhang, Q. Zhuge, H. Xin, Z. Xing, M. Xiang, S. Fan, et al., Design and analysis of high-speed optical access networks in the O-band with DSP-free ONUs and low-bandwidth optics, Opt. Express 26 (2018) 27873–27884.
[7] M. Tao, L. Zhou, H. Zeng, S. Li, X. Liu, 50-GB/s/λ TDM-PON based on 10G DML and 10G APD supporting PR10 link loss budget after 20-km downstream transmission in the O-band, in: Proc. Optical Fiber Communications Conference, 2017, Tu3G.2.
[8] J. Zhang, J.S. Wey, J. Yu, Z. Tu, B. Yang, et al., Symmetrical 50-Gb/s/λ PAM-4 TDM-PON in O-band with DSP and semiconductor optical amplifier supporting PR-30 link loss budget, in: Proc. Optical Fiber Communication Conference, 2018, M1B.4.
[9] M. Verbeke, P. Rombouts, H. Ramon, J. Verbist, J. Bauwelinck, X. Yin, G. Torfs, A 25 Gb/s all-digital clock and data recovery circuit for burst-mode applications in PONs, J. Lightw. Technol. 36 (2018) 1503–1509.
[10] J. Nakagawa, M. Nogami, N. Suzuki, M. Noda, S. Yoshima, H. Tagami, 10.3-Gb/s burst-mode 3R receiver incorporating full AGC optical receiver and 82.5-GS/s over-sampling CDR for 10G-EPON systems, IEEE Photon. Technol. Lett. 22 (2010) 471–473.
[11] M. Ishikawa, N. Suzuki, H. Tagami, S. Kozaki, A. Takahashi, A study of an over-sampling burst-mode CDR with gated VCO for 10Gbps PON systems, in: Proc. COIN, 2008, pp. 1–2.
[12] J. Terada, Y. Ohtomo, K. Nishimura, H. Katsurai, S. Kimura, N. Yoshimoto, Jitter-reduction and pulse-width-distortion compensation circuits for a 10Gb/s burst-mode CDR circuit, in: Proc. ISSCC, 2009, pp. 104–105.
[13] H. Tagami, S. Kozaki, K. Nakura, S. Kohama, M. Nogami, K. Motoshima, A burst-mode bit-synchronization IC with large tolerance for pulse-width distortion for gigabit ethernet PON, IEEE J. Solid-State Circuits 41 (2006) 2555–2565.
[14] P. Ossieur, J. Bauwelinck, X. Yin, C. Melange, B. Baekelandt, et al., A dual-rate burst-mode bit synchronization and data recovery circuit with fast optimum decision phase calculation, Int. J. Electron. Commun. 63 (2009) 931–938.
[15] A. Li, J. Faucher, D.V. Plant, Burst-mode clock and data recovery in optical multiaccess networks using broad-band PLLs, IEEE Photon. Technol. Lett. 18 (2006) 73–75.
[16] Y. Chang, First demonstration of a fast response/locking burst-mode physical-layer chipset for emerging 10G PON standards, in: Proc. ECOC, 2009, pp. 1–2.
[17] M. Oerder, H. Meyr, Digital filter and square timing recovery, IEEE Trans. Commun. 36 (1988) 605–612.
[18] C. Ting, J. Liang, A. Sheikholeslami, M. Kibune, H. Tamura, A blind baud-rate ADC-based CDR, IEEE J. Solid-State Circuits 48 (2013) 3285–3295.
[19] J. Zhang, X. Xiao, J. Yu, J.S. Wey, X. Huang, Z. Ma, Real-time FPGA demonstration of PAM-4 burst-mode all-digital clock and data recovery for single wavelength 50G PON application, in: Proc. Optical Fiber Communication Conference, 2018, M1B.7.
[20] J. Zhang, K. Wang, Y. Wei, L. Zhao, W. Zhou, et al., Symmetrical 50-Gb/s/λ PAM-4 TDM-PON at O-band supporting 26 db+ loss budget using low-bandwidth optics and semiconductor optical amplifier, in: Proc. Optical Fiber Communication Conference, 2020, Th1B.3.